How to cite: *Angew. Chem. Int. Ed.* **2023,** *62,* e202216021
International Edition: doi.org/10.1002/anie.202216021
German Edition: doi.org/10.1002/ange.202216021

Coordination Chemistry

An Aluminum Telluride with a Terminal Al=Te Bond and its Conversion to an Aluminum Tellurocarbonate by CO_2 Reduction

*Huihui Xu, Arseni Kostenko, Catherine Weetman, Shiori Fujimori, and Shigeyoshi Inoue**

Abstract: Facile access to dimeric heavier aluminum chalcogenides [(NHC)Al(Tipp)-μ-Ch]$_2$ (NHC = I*i*Pr (1,3-diisopropyl-4,5-dimethylimidazol-2-ylidene, IMe$_4$ (1,3,4,5-tetramethylimidazol-2-ylidene); Tipp = 2,4,6-*i*Pr$_3$C$_6$H$_2$; Ch = Se, Te) by treatment of NHC-stabilized aluminum dihydrides with elemental Se and Te is reported. The higher affinity of IMe$_4$ in comparison with I*i*Pr toward the Al center in [(NHC)Al(Tipp)-μ-Ch]$_2$ can be used for ligand exchange. Additionally, the presence of excess IMe$_4$ allows for cleavage of the dimers to form a rare example of a neutral multiply bonded heavier aluminum chalcogenide in the form of a tetracoordinate aluminum complex, (IMe$_4$)$_2$(Tipp)Al=Te. This species reacts with three equivalents of CO_2 across two Al–C^{NHC} and the Al=Te bond affording a pentacoordinate aluminum complex containing a dianionic tellurocarbonate ligand [CO_2Te]$^{2-}$, which is the first example of tellurium analogue of a carbonate [CO_3]$^{2-}$.

Introduction

Main group complexes with compositions ECh and E$_2$Ch$_3$ (E = Group 13, Ch = Group 16) are of high interest due to their electronic and optoelectronic properties, and their potential applications in innovative technologies.[1] It is, therefore, of high importance to understand their bonding motifs, electronic structure and aggregation processes to aid the development of advanced materials.[2] Aluminum chalcogenides are predominantly encountered in the form of alumina (Al_2O_3) which are used widely in ceramics, abrasives, refractory materials, and nonconductors.[3] Heavier aluminum chalcogenides (aluminum sulfides, selenides, and tellurides) have also attracted increasing attention, due to their applications in chemical vapor deposition (CVD), catalysis and materials.[4] Neutral multiply bonded heavier aluminum chalcogenides have been notoriously difficult synthetic targets.[5] Structural evidence of discrete molecular aluminum chalcogenides has been limited due to the polarized nature of terminal Al–Ch bonds (Figure 1, **I**) which makes them prone to head-to-tail self oligomerization, resulting in the corresponding tetramers (e.g. **II**) and dimers (e.g. **III**).

Only a few fully characterized tetramers, i.e. group 13 cubic chalcogenides of the composition [RECh]$_4$ (**II**), which have shown potential as precursors in the metal organic CVD,[6] have been reported (e.g. **IIa-c**).[7] As intermediates for the preparation of tetramers, dimers of the composition

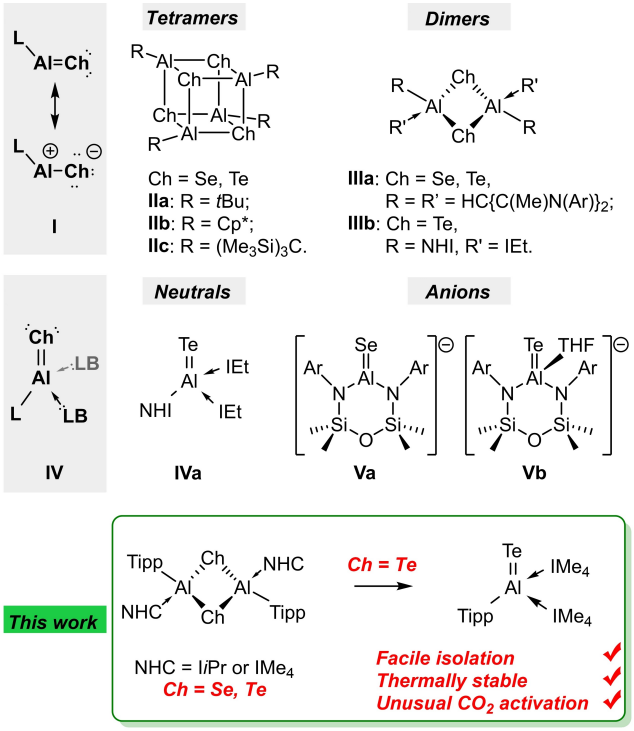

Figure 1. Selected heavier aluminum chalcogenides including tetramers, dimers, monomers (neutrals, anions) and this work. Ar = 2,6-*i*Pr$_2$C$_6$H$_3$; Cp* = C$_5$Me$_5$; NHI = 1,3-(2,6-diisopropylphenyl)-imidazol-2-imine; IEt = 1,3-diethyl-4,5-dimethylimidazol-2-ylidene; I*i*Pr = 1,3-diisopropyl-4,5-dimethylimidazol-2-ylidene; IMe$_4$ = 1,3,4,5-tetramethylimidazol-2-ylidene; Tipp = 2,4,6-*i*Pr$_3$C$_6$H$_2$.

[*] H. Xu, Dr. A. Kostenko, Dr. S. Fujimori, Prof. S. Inoue
School of Natural Sciences, Department of Chemistry, Catalysis Research Center and Institute of Silicon Chemistry, Technische Universität München
Lichtenbergstr. 4, 85748 Garching bei München (Germany)
E-mail: s.inoue@tum.de
Dr. C. Weetman
Department of Pure and Applied Chemistry
University of Strathclyde
295 Cathedral St, Glasgow G1 1XL Scotland (UK)

$[RR'ECh]_2$ (**III**),[1b,8] bearing ligands with increased steric demands in comparison to tetramers, have also been investigated.[9] In the case of the monomeric species, multiply bonded aluminum chalcogenides have been scarcely reported due to the lack of general synthetic routes and their inherent instability.[8d,9a,10] In those that have been isolated, Lewis acids or bases have been employed for kinetic and/or thermodynamic stabilization (e.g. **IV**).[2d,11] This was exemplified by our group in the case of the isolation of the first monomeric aluminum telluride $(IEt)_2Al(NHI)=Te$ **IVa** (IEt = 1,3-diethyl-4,5-dimethylimidazol-2-ylidene; NHI = 1,3-(2,6-diisopropylphenyl)-imidazol-2-imine), which contains a terminal Al=Te double bond.[9b] With the development of anionic aluminyl chemistry, wherein additional stabilization is achieved through interaction with alkali metals, this strategy has been employed for the isolation of discrete Al=Ch bonds.[12] For example, Coles and co-workers isolated $[Al=Se]^-$ (**Va**)[12e,13] and $[Al=Te]^-$ (**Vb**).[12c] With increased anionic character and nucleophilicity, both species showed remarkably nucleophilic reactivity towards Se and CO_2.[12c,13]

In light of our recent report on the stepwise isolation of aluminum sulfides,[11b] we sought to extend the aluminum chalcogenide chemistry to heavier analogues. Here, we present molecular heavier aluminum chalcogenides (Se, Te). Treatment of dimeric tellurides with NHC results in the isolation of a neutral aluminum telluride, $(IMe_4)_2Al(Tipp)=Te$ **5-Te**, containing a discrete Al=Te double bond. Interestingly, **5-Te** shows an unusual reactivity towards CO_2 forming a pentacoordinate aluminum complex **6-Te**, which contains an unprecedented tellurocarbonate $[CO_2Te]^{2-}$ moiety.

Results and Discussion

The synthesis of dimeric aluminum tellurides, $[IiPrAl(Tipp)-\mu-Te]_2$ **2-Te** and $[IMe_4Al(Tipp)-\mu-Te]_2$ **3-Te**, can be achieved by using the recently reported NHC-stabilized aluminum dihydrides $IiPrAl(Tipp)H_2$ **1-IiPr**[10a,11b] and $IMe_4Al(Tipp)H_2$ **1-IMe$_4$**. Unlike $(IEt)_2Al(NHI)=Te$ **IVa**, preparation of which was accomplished by using nBu_3PTe as Te source,[9b] nBu_3PTe was unreactive towards both aluminum dihydrides (even at 100 °C for 72 hours). Instead, reactions of **1-IiPr** or **1-IMe$_4$** with elemental tellurium at room temperature afforded the desired **2-Te** and **3-Te** in 60 % and 70 % yields, respectively (Scheme 1, path a and b). Using an analogous methodology, i.e. reactions of Se with **1-IiPr** or **1-IMe$_4$**, we were able to isolate **2-Se** and **3-Se** in high yields.

Single-crystal X-ray (SC-XRD) structures of **2-Te** and **3-Te** (Figure 2, Top and Middle) show aluminum centers possessing pseudo-tetrahedral geometry with the common chalcogen-bridged connectivity pattern of a four-membered Al_2Te_2 cycle, and the NHC ligands in a *trans* geometry. Al–Te bond lengths, 2.6051(5), 2.6363(5) Å in **2-Te** and 2.5974(9), 2.626(1) Å in **3-Te**, are very similar and closely resemble those of **IIIb** (2.6143(14), 2.6211(15) Å),[9b] but are somewhat longer than those observed in **IIIa** (2.575(3), 2.581(2) Å)[9a] as well as in related compounds reported by Roesky and co-workers (2.54–2.59 Å).[8a,c–e,14] The distances

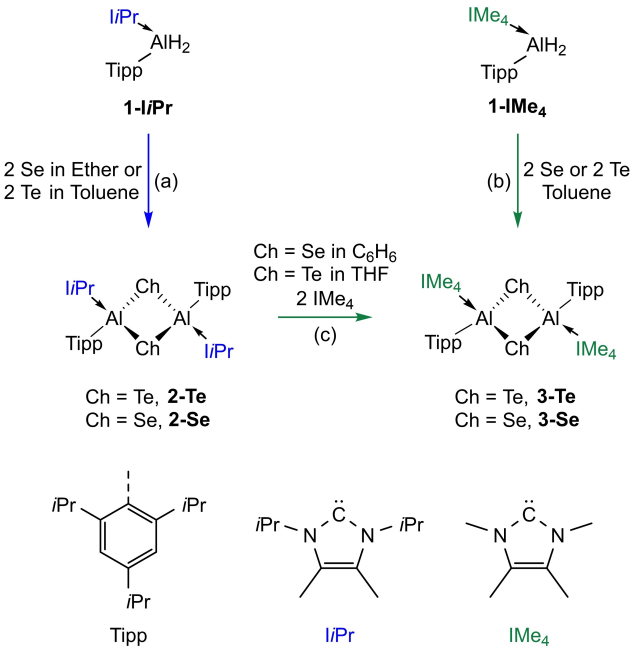

Scheme 1. Formation of **2-Te**, **2-Se**, **3-Te**, and **3-Se**.

of Al–C^{IMe4} (Al1–C16 2.062(3) Å) and Al–C^{Tipp} (Al1–C1 2.014(3) Å) in **3-Te** are noticeably shorter than those measured in **2-Te** (Al1–C16 2.099(2) Å; Al1–C1 2.022(1) Å), respectively. ^{125}Te NMR of **3-Te** exhibits a chemical shift at −954.2 ppm, which is in a higher field than that of **2-Te** (−898.0 ppm).

Although crystals of **2-Se** suitable for SC-XRD crystallography could not be obtained, its structure was confirmed by multinuclear NMR spectroscopy, elemental analysis (EA) and liquid injection field desorption ionization mass spectrometry (LIFDI-MS). The solid-state structure of **3-Se** (Figure 2, Bottom) exhibits a geometry similar to **3-Te** (Middle) featuring an $Al_2(\mu\text{-Se})_2$ core with the NHC and Tipp substituents bound to Al centers oriented in a *trans* fashion. Al1–Se1 bond length (2.386(1), 2.402(2) Å) is within the range of the typical Al–Se single bond length (2.34–2.54 Å) of reported aluminum selenides,[1b,2a,7a,b,d,8e,9a,15] but notably longer than the Al=Se double bond length (2.2032 (6) Å) of **Va**.[12e] ^{77}Se NMR of the IMe_4-substituted **3-Se** exhibits a chemical shift at −460.5 ppm, which is in a higher field than that of the IiPr-substituted **2-Se** (−355.7 ppm). Similar trend is observed for **2-Te** and **3-Te**. These observations imply a higher electron density at the chalcogen centers in the IMe_4-substituted complexes and may point to a preferential donicity of IMe_4 to the dimeric aluminum chalcogenides in comparison with IiPr. The electronic structures of the dimeric $[NHCAl(Tipp)-\mu-Ch]_2$ complexes were elucidated by density functional theory (DFT) calculations. The results and details of the computational methods are presented in the Supporting Information (Figures S73–S75, Tables S4 and S5).

Reactions of **2-Te** or **2-Se** with two equivalents of IMe_4 resulted in the NHC exchange reaction forming the respective complexes **3-Te** and **3-Se** (Scheme 1, path c). The

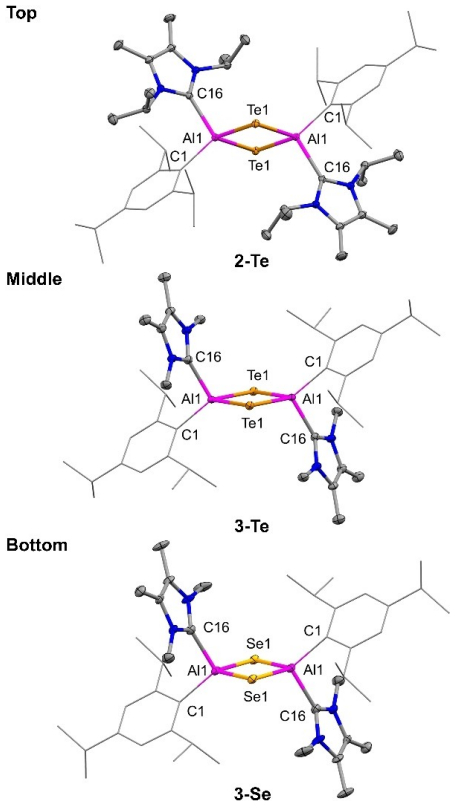

Figure 2. Molecular structures of **2-Te** (Top), **3-Te** (Middle), and **3-Se** (Bottom).[16] Ellipsoids are set at the 50% probability level; hydrogen atoms and co-crystallized solvent molecules are omitted for clarity and Tipp (2,4,6-*i*Pr$_3$C$_6$H$_2$) ligands are depicted in wireframe for simplicity. Selected bond lengths [Å] and angles [°]: **2-Te** Al1–Te1 2.6051(5), 2.6363(5), Al1–C1 2.022(1), Al1–C16 2.099(2), Al1–Te1–Al1 81.62(1). **3-Te** Al1–Te1 2.5974(9), 2.626(1), Al1–C1 2.014(3), Al1–C16 2.062(3), Al1–Te1–Al1 82.31(3). **3-Se** Al1–Se1 2.386(1), 2.402(2), Al1–C1 2.019(9), Al1–C16 2.078(5), Al1–Se1–Al1 80.56(5).

facile exchange of I*i*Pr by IMe$_4$ ligands indicates a higher affinity of IMe$_4$ toward the aluminum centers in the dimeric aluminum chalcogenide complexes. Indeed, the calculated free energy for IMe$_4$ dissociation from **3-Te** is by 8.0 kcal mol^{-1} higher than that of I*i*Pr dissociation from **2-Te** (23.0 vs. 15.0 kcal mol^{-1}). Similar values are calculated for **3-Se** and **2-Se** (24.5 and 13.7 kcal mol^{-1}). Contrary to this are the calculated gas phase proton affinities of I*i*Pr (280.3 kcal mol^{-1}) and IMe$_4$ (275.4 kcal mol^{-1}), which point to I*i*Pr being a better donor, due to the presence of the additional electron-donating alkyl groups. The relatively higher affinity of IMe$_4$ to the dimeric aluminum tellurides can be attributed to the steric effect - the repulsion is higher in the case of the bulkier I*i*Pr, as confirmed by natural steric analysis (Figure S76 in the Supporting Information). The lower steric repulsion results in higher affinity of IMe$_4$ toward the Al center in the dimeric complexes and enables the ligand exchange reaction. The steric effects of the differently substituted NHCs are also evident from the calculated energies of dissociation of **2-Te** and **3-Te** to the corresponding monomers with the respective Gibbs energies of 21.1 and 26.1 kcal mol^{-1} (27.3 kcal mol^{-1} for **2-Se** and 36.4 kcal mol^{-1} for **3-Se**).

Taking into account the above mentioned higher affinity of IMe$_4$ toward aluminum chalcogenides in comparison with I*i*Pr, we wanted to utilize this feature for preparation of the corresponding monomeric complexes featuring a terminal aluminum-tellurium bond. Interestingly, upon monitoring the above mentioned reaction of **2-Te** with IMe$_4$, that ultimately gives **3-Te** (Scheme 1, path c), the monomeric aluminum telluride I*i*Pr(IMe$_4$)Al(Tipp)=Te **4-Te** could be observed (Scheme 2, path a). Its formation was confirmed by multinuclear NMR spectroscopy and its composition was validated by LIFDI-MS (Figures S1–S6 in the Supporting Information). The ^{125}Te NMR signal appears at δ −924.7 ppm, which shifted upfield in comparison to the precursor (**2-Te**, δ −898.0 ppm). Calculations predict the formation of **4-Te** from **2-Te** to be exergonic by full 6.0 kcal mol^{-1} (Scheme 3, path b). Isolation of **4-Te** could not be accomplished since it subsequently and quantitatively converts to **3-Te** (Scheme 2, path b). Calculations predict this step to be exergonic by additional 2.8 kcal mol^{-1} (Scheme 3, path c).

Unlike **2-Te**, which in the presence of IMe$_4$ forms the detectible intermediate I*i*Pr(IMe$_4$)Al(Tipp)=Te **4-Te**, treatment of **2-Se** with IMe$_4$ only affords **3-Se**, and the corresponding intermediate **4-Se** could not be observed. This divergence can be explained by the relative energies of the intermediates involved in these reactions. Although the formation of **3-Te** and **3-Se** from **2-Te** and **2-Se** in the presence of IMe$_4$ is exergonic in both cases, by 8.8 and 11.6 kcal mol^{-1} respectively (Scheme 3 path a), the formation of intermediate **4** is only exergonic in the case of Te (−6.0 kcal mol^{-1} vs. 1.8 kcal mol^{-1} in the case of Se) (Scheme 3, path b). These calculations provide a plausible

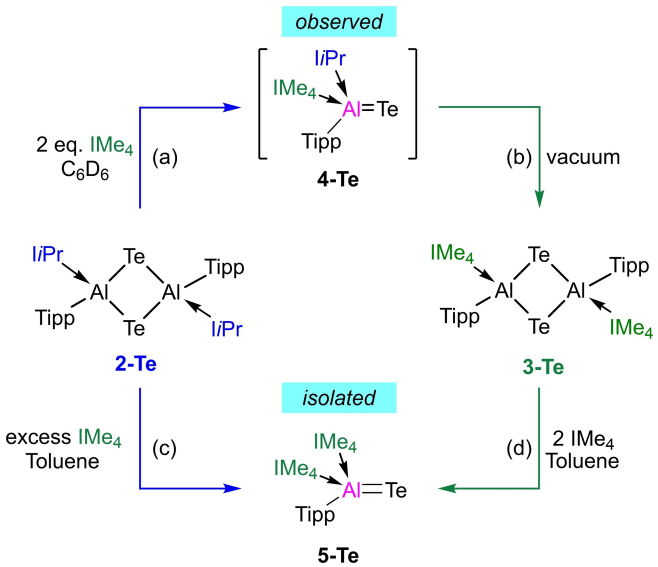

Scheme 2. Formation of **4-Te** and **5-Te**. I*i*Pr=1,3-diisopropyl-4,5-dimethylimidazol-2-ylidene; IMe$_4$=1,3,4,5-tetramethylimidazol-2-ylidene; Tipp=2,4,6-*i*Pr$_3$C$_6$H$_2$.

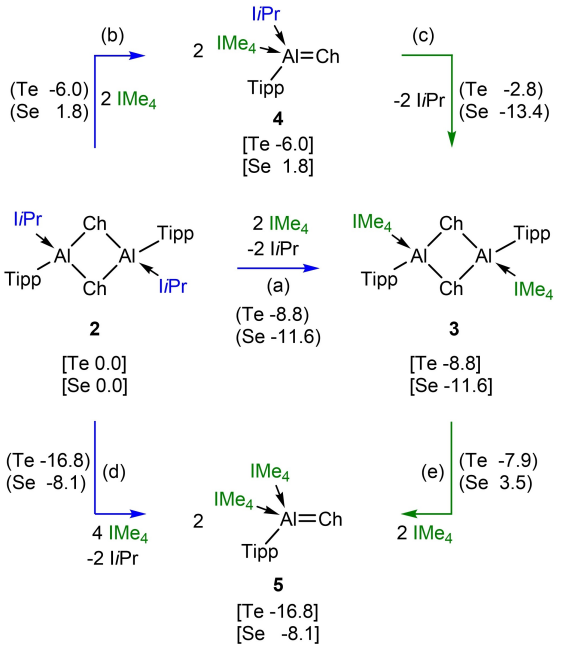

Scheme 3. Calculated energies (kcal mol^{-1}) for the reactions of **2**, **3**, **4** and **5**. Relative Gibbs energies of compounds are shown in square brackets. ΔG of reactions are shown in round brackets.

explanation of why intermediate **4-Se** could not be observed.

In attempt to actually isolate a monomeric aluminum telluride, we introduced IMe_4 in excess to **2-Te** (Scheme 2, path c), which furnished the aluminum telluride $(IMe_4)_2Al(Tipp)=Te$ **5-Te**, containing a tetracoordinate aluminum center and a terminal Al=Te bond, in a 45 % yield. **5-Te** could also be obtained in 63 % yield by introduction of two equivalents of IMe_4 to **3-Te** (Scheme 2, path d). To understand the formation of **5-Te**, Gibbs energy for the reaction of **2-Te** with four equivalents of IMe_4 to give two equivalents of **5-Te** and two equivalents of I*i*Pr was calculated giving $\Delta G = -16.8$ kcal mol^{-1} (Scheme 3, path d). Calculations indicate that **5-Te** is the most energetically favored species as its formation from **3-Te** and two equivalents of IMe_4 is also exergonic by 7.9 kcal mol^{-1} (Scheme 3, path e). However, preparation for the selenide analogue of **5-Te** by introduction of stoichiometric or excess amounts of IMe_4 to compound **2-Se** and **3-Se** did not yield the corresponding $(IMe_4)_2Al(Tipp)=Se$ **5-Se**. Unlike the formation of **5-Te** from **3-Te** in the presence of IMe_4, which was calculated to be exergonic by 7.9 kcal mol^{-1} (Scheme 3, path e), analogous formation of the hypothetical **5-Se** from **3-Se** is calculated to be endergonic by 3.5 kcal mol^{-1}. Although the formation of **5-Se** from **2-Se** is predicted to be exergonic by 8.1 kcal mol^{-1} (Scheme 3, path d), dissociation of IMe_4 and dimerization to **3-Se** energetically preferred by 3.5 kcal mol^{-1}. Thus, in the case of Te the most energetically favored compound is **5-Te**, while in the case of Se it is **3-Se**. This tendency could be explained by the higher proclivity for dimerization of Al–Se vs. Al–Te. This is evident from the dissociation energies of **3-Se** (36.4 kcal mol^{-1}) and **3-Te** (26.1 kcal mol^{-1}) to the corresponding monomers.

The single-crystal structure of **5-Te** (Figure 3) shows the Al center bound to the aryl substituent, two geminal IMe_4 ligands and a tellurium atom in a distorted tetrahedral manner. The Al1–Te1 distance of 2.534(1) Å is longer than those in **IVa** (2.5130 (14) Å),[9b] **Vb** (2.5039(7) Å)[12c] as well as the sum of covalent double bond radii ($\Sigma(r_2)=2.41$ Å),[17] although is shorter than the Al–Te single bond lengths in **2-Te** (2.605(5), 2.6363(5) Å) or **3-Te** (2.5974(9), 2.626(1) Å) and other dimeric aluminum tellurides (2.541–2.588 Å).[8d,9] The ^{125}Te NMR displays a signal at −1368.6 ppm, which is more shielded than that of dimeric **2-Te** (δ −898.0 ppm) and **3-Te** (δ −954.2 ppm) as well as monomeric **4-Te** (δ −924.7 ppm).

Selected frontier molecular orbitals of **5-Te** are presented in Figure 4. The HOMO-2 corresponds to the σ-type

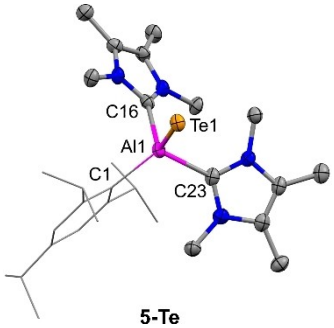

5-Te

Figure 3. Molecular structure of **5-Te**.[16] Ellipsoids are set at the 50 % probability level; hydrogen atoms and co-crystallized solvent molecules are omitted for clarity and Tipp (2,4,6-*i*Pr$_3$C$_6$H$_2$) ligands are depicted in wireframe for simplicity. Selected bond lengths [Å] and angles [°]: Al1–Te1 2.534(1), Al1–C1 2.047(4), Al1–C16 2.082(5), Al1–C23 2.061(5), Te1–Al1–C1 127.2(1), Te1–Al1–C16 108.2(1), Te1–Al1–C23 99.9(1).

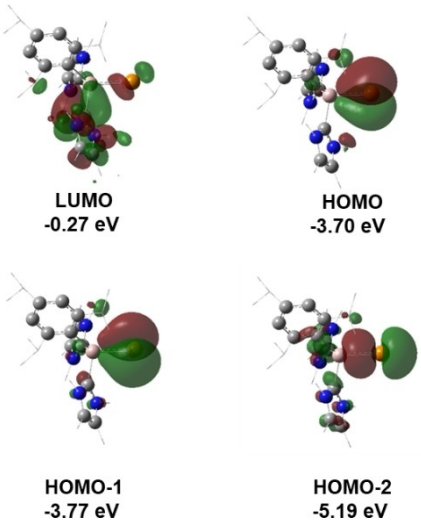

Figure 4. Selected molecular orbitals of **5-Te**. For clarity, hydrogens are omitted, and methyl and isopropyl substituents are shown as wireframes.

lone pair of Te and the σ-bond of Te–Al. The HOMO-1 and HOMO show π-type lone pairs extending toward Al center pointing to a higher bond order between Al and Te. The natural bond orbital (NBO) analysis shows a polarized Te–Al bonding interaction (68.7 % Te ($sp^{3.4}$), 31.3 % Al ($sp^{1.5}$)) with natural charges of −0.92 el. and +1.13 el. on Te and Al, respectively. Both Mayer bond order (MBO, 1.74) and Wiberg bond index (WBI, 1.17) indicate a double bond character of the Te–Al interaction. Second order perturbation theory analysis reveals donor-acceptor interactions (DAI) between one of the π-type lone pairs of Te and a lone vacancy p orbital of Al with occupancy of 0.36 el. (25.3 kcal mol^{-1}) and between the second π-type lone pair of Te and a lone-vacancy $sp^{4.0}$ orbital of Al with occupancy of 0.40 el. (13.0 kcal mol^{-1}). These interactions result in the double bond character of the Al–Te fragment. Additional details regarding the electronic structure of **5-Te** are presented in the Supporting Information (Figure S77).

Unlike **IVa**, for which the reactivity studies could not be carried out due to its instability, **5-Te** is thermally stable as there was no detectable change (^{1}H NMR) in THF-d_8 at 80 °C for at least 72 hours. Reaction of **5-Te** with BPh_3 resulted in elimination of the NHC ligand and formation of **3-Te** dimer (Scheme 4, path a). As chalcogen exchange have been shown to provide a route to isolation of terminal multiple chalcogen bonds,[18] we treated **5-Te** with lighter chalcogens. Reaction of **5-Te** with Se yielded the dimeric **3-Se** (Scheme 4, path b). This transformation presumably proceeds via the initial exchange of Te with Se, forming the transient intermediate **5-Se**, which cannot be isolated, due to its above described tendency to release IMe_4 and dimerize to **3-Se**. The reaction of **5-Te** with S_8 resulted in immediate decomposition with formation of metallic tellurium precipitate and ^{1}H NMR showing signals which correspond to TippH and IMe_4=S (Figure S9 in the Supporting Information).

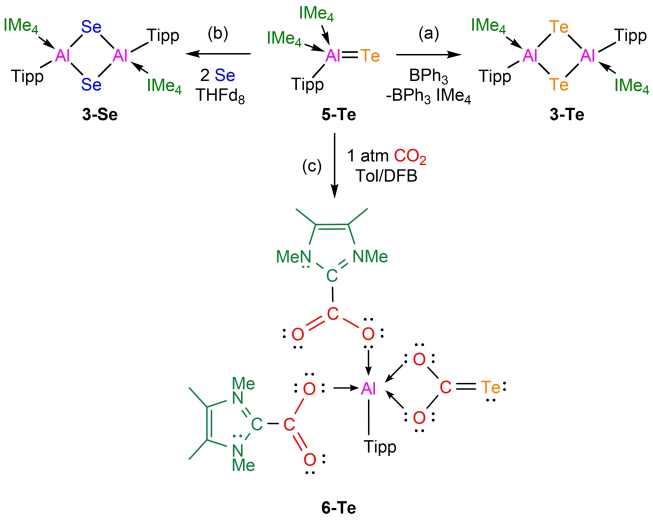

Scheme 4. Reactivity of **5-Te** towards BPh_3, Se and CO_2. IMe_4=1,3,4,5-tetramethylimidazol-2-ylidene; Tipp=2,4,6-iPr$_3$C$_6$H$_2$.

Attempts to study the reactivity of **5-Te** towards H_2, N_2O, CO, IMe_4-CO_2, tBu$_3$PSe, PPh_3, IMe_4-CuMes (Mes=2,4,6-Me$_3$C$_6$H$_2$), Diphenylacetylene, 2,6-Dimethylphenyl isocyanide, Phenylacetylene, Ph_2CO, Ni(COD)$_2$ (COD=1,5-cyclooctadiene), MesCu, Benzophenone, NMO (4-Methylmorpholine *N*-oxide), Me_2S-AuCl and Mes_2Fe were unsuccessful (Figure S11 in the Supporting Information). As mentioned in the introduction, the reaction of CO_2 with [Al=Se]$^-$ **Va** and [Al=Te]$^-$ **Vb** resulted in a single CO_2 insertion product, [Al(NON^{Dipp})(SeC{O}O)]$^-$ (NON^{Dipp}=[O(SiMe$_2$NDipp)$_2$]$^{2-}$, Dipp=2,6-iPr$_2$C$_6$H$_3$),[13] and a double CO_2 insertion product, [Al(NON^{Dipp})({OC(O)}$_2$Te)]$^-$,[12c] respectively. Here, however, exposure of **5-Te** to CO_2 results in the formation of a triple CO_2 insertion product (Scheme 4, path c), which was identified as $(IMe_4CO_2)_2$Al-(Tipp)-μ-O$_2$C=Te (**6-Te**). Formally, three equivalents of CO_2 reacted with **5-Te** across two Al–C^{NHC} bonds and the terminal Al=Te bond. We note here that there was no observed reactivity between CO_2 and the dimeric species **2-Te**, **2-Se**, **3-Te**, or **3-Se** even at 80 °C.

The solid-state structure of **6-Te** (Figure 5A) shows that the pentacoordinate Al center, bound to the Tipp substituent, two CO_2–NHC (η^1-κ*O*) moieties and CO_2Te (η^2-κ*O*,*O*′), adopts a distorted trigonal bipyramidal geometry. The

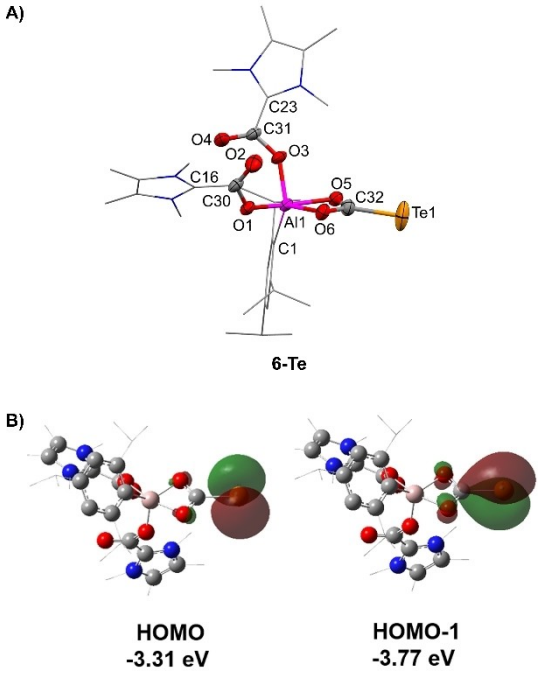

Figure 5. A) Molecular structure of **6-Te**.[16] Ellipsoids are set at the 50 % probability level; hydrogen atoms and co-crystallized solvent molecules are omitted for clarity and the Tipp (2,4,6-iPr$_3$C$_6$H$_2$) ligand is depicted in wireframe for simplicity. Selected bond lengths [Å] and angles [°]: C32–Te1 2.088(5), Al1–O1 1.865(4), Al1–O3 1.824(3), Al1–O5 2.028(4), Al1–O6 1.871(4), Al1–C1 1.992(5), C30–O1 1.288(6), C30–O2 1.221(7), C32–O5 1.268(7), C32–O6 1.317(7), C31–O3 1.294(6), C31–O4 1.211(6), C23–C31 1.474(7), C16–C30 1.546(16), O5–C32–O6 113.4(4), O5–Al1–O6 67.16(15). B) Selected Molecular orbitals of **6-Te**. For clarity, hydrogens are omitted, and methyl and isopropyl substituents are shown as wireframes.

corresponding structural parameters in a μ-CO_2-$\kappa^2O,O':\kappa C$ fashion[19] are comparable to previous examples[20] involving Al^{I}[21] and Al^{III}[22] bimetallic precursors. Bond lengths of Al1–O1 (1.865(4) Å), Al1–O3 (1.824(3) Å), Al1–O6 (1.871 (4) Å) are within the range of typical Al–O single bond (ca. 1.87 Å),[23] whereas Al1–O5 (2.028(4) Å) is notably longer than this single bond length. C–O bond lengths for the Al–μ–O_2C–Te unit (C32–O5 1.268(7) Å, C32–O6 1.317 (7) Å) fall between the typical ranges for C–O single and double bonds,[24] supporting the idea of a formal two-electron reduction of CO_2 and being consistent with delocalization of the π-electron density over the entirety of the CO_2 fragment. The C32–Te1 distance of 2.088(5) Å is slightly longer than the average C=Te length (ca. 1.93 Å)[25] and still shorter than an average of typical C–Te single bond (ca. 2.158 Å).[26] In ^{13}C NMR, the carbon of the terminal C=Te bond appears at δ 226.56 ppm, which is more shielded than those of typical telluroketones with terminal C=Te double bond (^{13}C NMR: δ 284.00–351.00 ppm),[27] but more deshielded than measured in NHC supported telluroketones (δ 126.00–187.00 ppm).[25,28] The ^{125}Te NMR signal appears at a higher chemical shift (δ −187.6 ppm) than that of **5-Te** (δ −1368.6 ppm), but it is more shielded than the resonance measured for [Al(NON^{Dipp})({OC(O)}$_2$Te)]$^-$ (CO_2 activation product of **Vb**, δ −17.80 ppm)[12c] and significantly more deshielded for the complex containing terminal Si=Te (δ −1010.4 or −982.5 ppm).[29]

The DFT calculated Gibbs energy for reaction of **5-Te** with three molecules of CO_2 to give **6-Te** is −23.4 kcal mol^{-1}. Calculated energies of the possible intermediates (Figure S78 in the Supporting Information) indicate that the reaction most likely proceeds via two initial CO_2 insertions into the Al–C^{NHC} bond with the third addition across the Al=Te bond taking place at the last step. WBI and MBO of 1.19 and 1.39 indicate a multiple bond character of the C–Te interaction.

The NBO analysis shows a polarized Te1 (34.8 %)–C (65.2 %) bonding interaction. Additionally, the Te center contains one σ-type and two π-type lone pairs. The π-type lone pairs correspond to HOMO-1 and HOMO (Figure 5B), with the former extending toward the carbon center. The second order perturbation analysis shows a significant DAI between the Te lone pair and the p-orbital of the carbon of 223.4 kcal mol^{-1}, which is of higher magnitude than the DAIs between the lone pair of the oxygens and the empty p orbital of the carbon (191.6 and 153.1 kcal mol^{-1}), resulting in Te–C with multiple bond character. Inquiry into the bonding situation around the Al center reveals essentially dative interactions between Al and the κ^2-coordinated CO_2Te and the κ^1-coordinated NHC–CO_2 moieties. The calculated WBIs and MBOs show rather weak bonding between Al and the oxygen atoms of the CO_2Te and NHC–CO_2 substituent, with Al1–O1 (0.24, 0.60), Al1–O3 (0.28, 0.70), Al1–O5 (0.26, 0.69), Al1–O6 (0.30, 0.79) (Figure 6a). Each of the oxygen atoms bonded to Al (O1, O3, O5 and O6) contains three lone pairs that are donated into the lone-vacancy orbitals of Al. Detailed NBO analysis and additional features of the electronic structure of **6-Te** are presented in the Supporting Information (Figures S79–81,

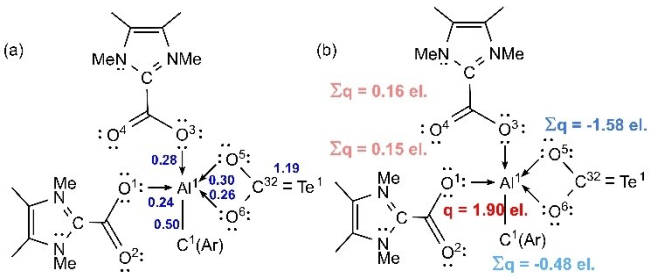

Figure 6. a) Selected WBI in **6-Te**; b) Distribution of natural charge in **6-Te**.

Table S6). Most of the positive natural charge resides on Al (+1.90 el.), while the NHC-CO_2 moieties are almost neutral (Σq = +0.16 and +0.15 el.). Most of the negative charge is concentrated on the CO_2Te moiety with Σq = −1.58 el. and remaining −0.48 el. reside on the aryl substituent.

Thus the DFT calculations suggest that the CO_2Te moiety in **6-Te** can be described as tellurocarbonate $[CO_2Te]^{2-}$, which is the first example of a tellurium analogue of a carbonate $[CO_3]^{2-}$. Carbonate is a ubiquitous ligand in transition metal chemistry. A few examples of alkali metal, alkaline earth metal and main-group-element complexes coordinated by carbonates also have been reported.[30] However, to the best of our knowledge, there are no examples of complexes substituted by heavy carbonate analogues. The preferred mode of coordination of the tellurocarbonate to aluminum center is via the two oxygen atoms, as calculations show that the isolated (tellurocarbonate-κ^2 O,O′)Al isomer is by 5.2 kcal mol^{-1} more energetically favored than the hypothetical (tellurocarbonate-κ^2 O,Te)Al isomer. In general, contrary to carbonyl (C=O) and thiocarbonyl compounds (C=S), compounds with heavier terminal C=Ch bonds[25,27c,31] have been much less explored because of their high reactivity. In the case of tellurium it can be ascribed to the unfavorable C_{2p}–Te_{5p} orbital overlap,[32] and strong tendency for oligomerization, isomerization into singly bonded molecules, or decomposition into simpler entities.[33] But, while C=O and C=S are ubiquitous building blocks in nature and have been explored for their uses from the chemical industry to bioscience,[34] the potential of heavier C=Ch in the context of biological functionalities is yet to be unveiled. In terms of the reactivity exploration of **6-Te**, this compound features poor solubility in benzene, toluene, acetonitrile, THF and pyridine, but is soluble in 1,2-difluorobenzene. **6-Te** is thermally unstable, and decomposes even at −30 °C to IMe_4=Te, IMe_4-CO_2 and unidentified species (Figure S12–S16, in the Supporting Information). Due to the poor solubility and inherent thermal instability of **6-Te**, our attempts to study its reactivity towards a variety of reagents (i.e. IMe_4, cAAC^{Me} (1-(2,6-*i*Pr$_2$C$_6$H$_3$)-3,3,5,5-tetramethylpyrrolidin-2-ylidene), $Na_2Fe(CO)_4$, BPh_3, PPh_3, KOTf, KC_8, diphenylacetylene, styrene, ethylene, hydrogen) have been unsuccessful so far. (Figure S17–19, in the Supporting Information).

Conclusion

In summary, we have isolated a series of dimeric aluminum tellurides and selenides and a monomeric aluminum telluride **5-Te**, which bears a terminal Al=Te double bond. Attempts to isolate the analogous monomeric aluminum selenide containing an Al=Se double bond were unsuccessful due to its preference to form thermodynamically more favorable dimeric species, as confirmed by DFT calculations. In contrast to our previously reported aluminum telluride (**IVa**), **5-Te** features better stability that enables its reactivity studies towards small molecules. Reaction of elemental Se results in the lighter dimeric species via an inferred transient aluminum selenide with a terminal Al–Se bond. Most interestingly, the reactivity of **5-Te** towards CO_2 results a triple CO_2 insertion product **6-Te** with an unusual pentacoordinate aluminum center. It possesses a tellurocarbonate moiety with a terminal C=Te double bond, representing a unique case of tellurium analogue of a carbonate ligand. Numerous attempts to study further reactivity of the dimeric species, **5-Te** or **6-Te**, towards unsaturated substrates and transition metals have been unsuccessful thus far, however the research of synthetic capabilities of these and similar systems is ongoing in our group.

Acknowledgements

We are grateful to the European Research Council (ALLOWE 101001591) for financial support. H.X. gratefully acknowledges financial support from the China Scholarship Council (CSC). C.W. is thankful to the University of Strathclyde for the award of a Chancellor's Fellowship. We thank Dr. Franziska Hanusch for the SC-XRD measurements, Ivan Antsiburov and Maximilian Muhr for the LIFDI-MS measurements. The authors gratefully acknowledge the Leibniz Supercomputing Centre for funding this project by providing computing time on its Linux-Cluster. Open Access funding enabled and organized by Projekt DEAL.

Conflict of Interest

The authors declare no conflict of interest.

Data Availability Statement

The data that support the findings of this study are available in the Supporting Information of this article.

Keywords: Aluminum Selenide · Aluminum Telluride · CO_2 Activation · Chalcogen · Tellurocarbonate

[1] a) G. Bai, H. W. Roesky, J. Li, M. Noltemeyer, H.-G. Schmidt, *Angew. Chem. Int. Ed.* **2003**, *42*, 5502–5506; *Angew. Chem.* **2003**, *115*, 5660–5664; b) C. Schnitter, A. Klemp, H. W. Roesky, H.-G. Schmidt, C. Röpken, R. Herbst-Irmer, M. Noltemeyer, *Eur. J. Inorg. Chem.* **1998**, 2033–2039; c) K. A. Evans in *The Chemistry of Aluminium, Indium and Gallium* (Ed.: A. J. Downs), Blackie Academic & Professional, Glasgow, **1993**, p. 248.

[2] a) C. Cui, H. W. Roesky, H. Hao, H.-G. Schmidt, M. Noltemeyer, *Angew. Chem. Int. Ed.* **2000**, *39*, 1815–1817; *Angew. Chem.* **2000**, *112*, 1885–1887; b) J. Hicks, A. Heilmann, P. Vasko, J. M. Goicoechea, S. Aldridge, *Angew. Chem. Int. Ed.* **2019**, *58*, 17265–17268; *Angew. Chem.* **2019**, *131*, 17425–17428; c) M. D. Anker, M. P. Coles, *Angew. Chem. Int. Ed.* **2019**, *58*, 18261–18265; *Angew. Chem.* **2019**, *131*, 18429–18433; d) C. Weetman, H. Xu, S. Inoue in *Encyclopedia of Inorganic and Bioinorganic Chemistry* (Ed.: R. A. Scott), Wiley, Hoboken, **2020**, pp. 1–20.

[3] a) D. Neculai, H. W. Roesky, A. M. Neculai, J. Magull, B. Walfort, D. Stalke, *Angew. Chem. Int. Ed.* **2002**, *41*, 4294–4296; *Angew. Chem.* **2002**, *114*, 4470–4472; b) M. R. Mason, J. M. Smith, S. G. Bott, A. R. Barron, *J. Am. Chem. Soc.* **1993**, *115*, 4971–4984; c) R. J. Wehmschulte, P. P. Power, *J. Am. Chem. Soc.* **1997**, *119*, 8387–8388.

[4] A. R. Barron, *Adv. Mater. Opt. Electron.* **1995**, *5*, 245–258.

[5] P. Bag, C. Weetman, S. Inoue, *Angew. Chem. Int. Ed.* **2018**, *57*, 14394–14413; *Angew. Chem.* **2018**, *130*, 14594–14613.

[6] a) M. G. Simmonds, W. L. Gladfelter, *The Chemistry of Metal CVD*, Wiley, New York, **1994**, pp. 45–103; b) M. B. Power, A. R. Barron, D. Hnyk, H. E. Robertson, D. W. H. Rankin, *Adv. Mater. Opt. Electron.* **1995**, *5*, 177–185.

[7] a) A. H. Cowley, R. A. Jones, P. R. Harris, D. A. Atwood, L. Contreras, C. J. Burek, *Angew. Chem. Int. Ed. Engl.* **1991**, *30*, 1143–1145; *Angew. Chem.* **1991**, *103*, 1164–1166; b) S. Schulz, H. W. Roesky, H. J. Koch, G. M. Sheldrick, D. Stalke, A. Kuhn, *Angew. Chem. Int. Ed. Engl.* **1993**, *32*, 1729–1731; *Angew. Chem.* **1993**, *105*, 1828–1830; c) K. S. Klimek, J. Prust, H. W. Roesky, M. Noltemeyer, H.-G. Schmidt, *Organometallics* **2001**, *20*, 2047–2051; d) C. J. Harlan, E. G. Gillan, S. G. Bott, A. R. Barron, *Organometallics* **1996**, *15*, 5479–5488.

[8] a) M. G. Gardiner, C. L. Raston, V.-A. Tolhurst, *J. Chem. Soc. Chem. Commun.* **1995**, 2501–2502; b) W. J. Grigsby, C. L. Raston, V.-A. Tolhurst, B. W. Skelton, A. H. White, *J. Chem. Soc. Dalton Trans.* **1998**, 2547–2556; c) H. Zhu, J. Chai, H. W. Roesky, M. Noltemeyer, H.-G. Schmidt, D. Vidovic, J. Magull, *Eur. J. Inorg. Chem.* **2003**, 3113–3119; d) C. Cui, H. W. Roesky, M. Noltemeyer, H.-G. Schmidt, *Inorg. Chem.* **2000**, *39*, 3678–3681; e) C. Cui, H. W. Roesky, M. Noltemeyer, H.-G. Schmidt, *Organometallics* **1999**, *18*, 5120–5123.

[9] a) V. Jancik, M. M. Moya Cabrera, H. W. Roesky, R. Herbst-Irmer, D. Neculai, A. M. Neculai, M. Noltemeyer, H.-G. Schmidt, *Eur. J. Inorg. Chem.* **2004**, 3508–3512; b) D. Franz, T. Szilvasi, E. Irran, S. Inoue, *Nat. Commun.* **2015**, *6*, 10037.

[10] a) C. Weetman, A. Porzelt, P. Bag, F. Hanusch, S. Inoue, *Chem. Sci.* **2020**, *11*, 4817–4827; b) P. Bag, A. Porzelt, P. J. Altmann, S. Inoue, *J. Am. Chem. Soc.* **2017**, *139*, 14384–14387; c) R. L. Falconer, K. M. Byrne, G. S. Nichol, T. Krämer, M. J. Cowley, *Angew. Chem. Int. Ed.* **2021**, *60*, 24702–24708; *Angew. Chem.* **2021**, *133*, 24907–24913; d) C. Bakewell, K. Hobson, C. J. Carmalt, *Angew. Chem. Int. Ed.* **2022**, *61*, e202205901; *Angew. Chem.* **2022**, *134*, e202205901.

[11] a) D. Franz, S. Inoue, *Dalton Trans.* **2016**, *45*, 9385–9397; b) H. Xu, C. Weetman, F. Hanusch, S. Inoue, *Chem. Eur. J.* **2022**, *28*, e202104042.

[12] a) J. Hicks, P. Vasko, J. M. Goicoechea, S. Aldridge, *Nature* **2018**, *557*, 92–95; b) R. J. Schwamm, M. D. Anker, M. Lein, M. P. Coles, *Angew. Chem. Int. Ed.* **2019**, *58*, 1489–1493; *Angew. Chem.* **2019**, *131*, 1503–1507; c) M. J. Evans, M. D. Anker, C. L. McMullin, N. A. Rajabi, M. P. Coles, *Chem. Commun.* **2021**, *57*, 2673–2676; d) T. X. Gentner, R. E. Mulvey,

Angew. Chem. Int. Ed. **2021**, *60*, 9247–9262; *Angew. Chem.* **2021**, *133*, 9331–9348; e) M. D. Anker, M. P. Coles, *Angew. Chem. Int. Ed.* **2019**, *58*, 13452–13455; *Angew. Chem.* **2019**, *131*, 13586–13589.
[13] M. J. Evans, M. D. Anker, C. L. McMullin, S. E. Neale, N. A. Rajabi, M. P. Coles, *Chem. Sci.* **2022**, *13*, 4635–4646.
[14] W. Uhl, U. Schütz, *Z. Naturforsch. B* **1994**, *49*, 931–934.
[15] W. Uhl, R. Gerding, I. Hahn, S. Pohl, W. Saak, H. Reuter, *Polyhedron* **1996**, *15*, 3987–3992.
[16] Deposition Numbers 2215503 (for **2-Te**), 2215504 (for **3-Se**), and 2215505 (for **3-Te**), 2215506 (for **5-Te**), 2215507 (for **6-Te**) contain the supplementary crystallographic data for this paper. These data are provided free of charge by the joint Cambridge Crystallographic Data Centre and Fachinformationszentrum Karlsruhe Access Structures service.
[17] P. Pyykkö, M. Atsumi, *Chem. Eur. J.* **2009**, *15*, 12770–12779.
[18] D. Sarkar, D. Wendel, S. U. Ahmad, T. Szilvasi, A. Pothig, S. Inoue, *Dalton Trans.* **2017**, *46*, 16014–16018.
[19] C. Yoo, Y. Lee, *Chem. Sci.* **2017**, *8*, 600–605.
[20] H. Corona, M. Pérez-Jiménez, F. de la Cruz-Martínez, I. Fernández, J. Campos, *Angew. Chem. Int. Ed.* **2022**, *61*, e202207581; *Angew. Chem.* **2022**, *134*, e202207581.
[21] a) J. Hicks, A. Mansikkamaki, P. Vasko, J. M. Goicoechea, S. Aldridge, *Nat. Chem.* **2019**, *11*, 237–241; b) C. McManus, J. Hicks, X. Cui, L. Zhao, G. Frenking, J. M. Goicoechea, S. Aldridge, *Chem. Sci.* **2021**, *12*, 13458–13468; c) H.-Y. Liu, R. J. Schwamm, M. S. Hill, M. F. Mahon, C. L. McMullin, N. A. Rajabi, *Angew. Chem. Int. Ed.* **2021**, *60*, 14390–14393; *Angew. Chem.* **2021**, *133*, 14511–14514; d) D. Sorbelli, L. Belpassi, P. Belanzoni, *J. Am. Chem. Soc.* **2021**, *143*, 14433–14437; e) M. M. D. Roy, J. Hicks, P. Vasko, A. Heilmann, A.-M. Baston, J. M. Goicoechea, S. Aldridge, *Angew. Chem. Int. Ed.* **2021**, *60*, 22301–22306; *Angew. Chem.* **2021**, *133*, 22475–22480.
[22] S. Sinhababu, M. R. Radzhabov, J. Telser, N. P. Mankad, *J. Am. Chem. Soc.* **2022**, *144*, 3210–3221.
[23] a) G. I. Shcherbakova, M. K. Shaukhin, A. D. Kirilin, P. A. Storozhenko, *Russ. Chem. Bull.* **2021**, *70*, 1275–1280; b) Z. Sun, H. Wang, Y. Zhang, J. Li, Y. Zhao, W. Jiang, L. Wang, *Dalton Trans.* **2013**, *42*, 12956–12964.
[24] a) N. T. Thuy Tran, S.-Y. Lin, O. E. Glukhova, M.-F. Lin, *RSC Adv.* **2016**, *6*, 24458–24463; b) A. Walsh, *Trans. Faraday Soc.* **1946**, *42*, 56–62.
[25] N. Kuhn, G. Henkel, T. Kratz, *Chem. Ber.* **1993**, *126*, 2047–2049.
[26] F. H. Allen, O. Kennard, D. G. Watson, L. Brammer, A. G. Orpen, R. Taylor, *J. Chem. Soc. Perkin Trans. 2* **1987**, S1–S19.
[27] a) M. Minoura, T. Kawashima, N. Tokitoh, R. Okazaki, *Chem. Commun.* **1996**, 123–124; b) Y. Mutoh, N. Kozono, K. Ikenaga, Y. Ishii, *Coord. Chem. Rev.* **2012**, *256*, 589–605; c) M. Minoura, T. Kawashima, R. Okazaki, *J. Am. Chem. Soc.* **1993**, *115*, 7019–7020.
[28] a) S. T. Manjare, S. Sharma, H. B. Singh, R. J. Butcher, *J. Organomet. Chem.* **2012**, *717*, 61–74; b) D. Rottschäfer, D. E. Fuhs, B. Neumann, H.-G. Stammler, R. S. Ghadwal, *Z. Anorg. Allg. Chem.* **2020**, *646*, 574–579.
[29] a) S. Yao, Y. Xiong, M. Brym, M. Driess, *Chem. Asian J.* **2008**, *3*, 113–118; b) S. Yao, Y. Xiong, M. Driess, *Chem. Eur. J.* **2010**, *16*, 1281–1288.
[30] a) S. E. Wolf, L. Müller, R. Barrea, C. J. Kampf, J. Leiterer, U. Panne, T. Hoffmann, F. Emmerling, W. Tremel, *Nanoscale* **2011**, *3*, 1158–1165; b) C. Sanloup, J. M. Hudspeth, V. Afonina, B. Cochain, Z. Konôpková, G. Lelong, L. Cormier, C. Cavallari, *Front. Earth Sci.* **2019**, *7, 72*.
[31] M. Minoura, T. Kawashima, R. Okazaki, *Tetrahedron Lett.* **1997**, *38*, 2501–2504.
[32] M. Minoura, T. Kawashima, N. Tokitoh, R. Okazaki, *Phosphorus Sulfur Silicon Relat. Elem.* **1998**, *136*, 549–552.
[33] N. B. Jaufeerally, H. H. Abdallah, P. Ramasami, H. F. Schaefer, *J. Phys. Chem. A* **2013**, *117*, 5567–5577.
[34] a) N. Kuhn, G. Verani, *Handbook of Chalcogen Chemistry: New Perspectives in Sulfur, Selenium and Tellurium*, The Royal Society of Chemistry, London, **2007**, pp. 107–144; b) N. B. Jaufeerally, P. Ramasami, P. Jerabek, G. Frenking, *J. Mol. Model.* **2014**, *20*, 2433; c) E. R. T. Tiekink, *Dalton Trans.* **2012**, *41*, 6390–6395.

Manuscript received: October 31, 2022
Accepted manuscript online: January 12, 2023
Version of record online: February 6, 2023